



This is a repository copy of *Assessment of rail grinding maintenance surface quality and damage propagation in subsequent loading cycles for premium rail grades.*

White Rose Research Online URL for this paper:

<https://eprints.whiterose.ac.uk/202339/>

Version: Published Version

Article:

Mesaritis, M. orcid.org/0000-0002-1724-5958, Cuervo, P., Santa, J.F. et al. (2 more authors) (2023) Assessment of rail grinding maintenance surface quality and damage propagation in subsequent loading cycles for premium rail grades. *Wear*, 530-531. 205051. ISSN 0043-1648

<https://doi.org/10.1016/j.wear.2023.205051>

Reuse

This article is distributed under the terms of the Creative Commons Attribution (CC BY) licence. This licence allows you to distribute, remix, tweak, and build upon the work, even commercially, as long as you credit the authors for the original work. More information and the full terms of the licence here:

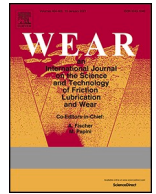
<https://creativecommons.org/licenses/>

Takedown

If you consider content in White Rose Research Online to be in breach of UK law, please notify us by emailing eprints@whiterose.ac.uk including the URL of the record and the reason for the withdrawal request.



eprints@whiterose.ac.uk
<https://eprints.whiterose.ac.uk/>



Assessment of rail grinding maintenance surface quality and damage propagation in subsequent loading cycles for premium rail grades

M. Mesaritis^{a,*}, P. Cuervo^b, J.F. Santa^b, A. Toro^b, R. Lewis^a

^a Leonardo Centre for Tribology, Department of Mechanical Engineering, University of Sheffield, Sheffield, UK

^b Grupo de Tribología y Superficies, Universidad Nacional de Colombia, Medellín, Colombia

ARTICLE INFO

Keywords:

Rail grinding
Post-grinding performance
Rolling-contact fatigue
WEL

ABSTRACT

Rail samples were tested under various scenarios as part of a complete analysis of the rail grinding process. Two main groups of tests were performed which assessed the following: 1) preventive and corrective maintenance on fresh rail samples and 2) post-grinding tribological performance of the ground samples. The results allowed further knowledge to be acquired with regards to the performance and effectiveness of the grinding process and its effect on the surface quality of the rail samples. Results indicated a correlation between White Etching Layer and the formation of cracks and defects. Additionally, the harder grades were found to retain larger quantities of White Etching Layer upon completion of the rolling/sliding testing due to the hardness gradient between the White Etching Layer and bulk material, promoting the formation of cracks.

1. Introduction

Under normal usage, rails show signs of wear and Rolling Contact Fatigue (RCF). The resistance against both RCF and wear depends upon the rail grade, its hardness and microstructure. Rail grinding is utilised to remove any defects which occur due to RCF or wear. However, sub-optimal grinding can occur due to limited resources and time on track. Hence, it is important to find the optimum combination for the grinding conditions, such as the depth of material to remove and the interval between the successive operations. Depending on the rail condition, a preventive or corrective grinding process is performed.

1.1. Rail maintenance types

In preventive maintenance, rail grinding is used to shorten RCF cracks in the rail, reducing the likelihood of the cracks growing to a point at which they effect the structural integrity of the rail. The material to be removed should be minimal and there are specific operational parameters applied for the current process. This rail grinding procedure is planned in advance with a defined depth of metal removal. Usually, the maintenance plan is based on the track usage and crack growth. Furthermore, it is important to find the ideal conditions in this type of maintenance to avoid being over-conservative, which might lead to excessive material loss. According to Grassie et al. [1] the appropriate

preventive maintenance schedule can achieve a 40% reduction on the total cost of the grinding along with the cost of rail replacement, while the reliability of the track and the rail can be improved significantly.

Corrective maintenance needs to be executed in cases where the rail profiles have become significantly deformed. As a result, rail grinding needs to be undertaken with different parameters so that it will be able to remove additional material and restore the rails back to their required/designed profile. This type of maintenance is not planned in advance and is usually executed after rail inspections. In corrective maintenance, larger amounts of material are usually removed compared to preventive maintenance.

1.2. Premium rail grades

Further to tackling defects and normal wear through rail grinding, rail manufacturers achieved increased resistance against both RCF and wear, by developing premium rail grades through thermal hardening and/or by alloying. The lamellar mixture of ferrite and cementite in pearlite makes it capable of absorbing part of applied forces by increasing its ductility and elasticity [2]. The interlamellar spacing within the pearlite and the grain size is controlled by the cooling rate during the manufacturing process. A slow cooling procedure will result in a coarser structure (larger grains) compared to a rapid cooling. Higher hardness usually occurs with rapid cooling and finer grain sizes. In the

* Corresponding author.

E-mail address: mmesaritis1@sheffield.ac.uk (M. Mesaritis).

<https://doi.org/10.1016/j.wear.2023.205051>

Received 26 February 2023; Received in revised form 26 June 2023; Accepted 6 July 2023

Available online 8 July 2023

0043-1648/© 2023 The Authors. Published by Elsevier B.V. This is an open access article under the CC BY license (<http://creativecommons.org/licenses/by/4.0/>).

railway industry the hardness levels define the grade of the rail materials e.g. A minimum hardness of 260HB is measured for the R260 rail grade and the premium rail grade R350HT hardness a lowest hardness of around 350HB [3].

In previous work [4] a demonstration of a laboratory grinding technique on R260 rail material was presented along with results with regards to the rail samples' microstructure and hardness. This testing, also known as twin-disc testing was performed by pressing two discs against each other, to achieve the desired contact pressure, and by generating a relative motion between the two surfaces. This allowed the reproduction of the rolling/sliding conditions that exist between the wheel and the rail. An attempt was made to correlate the wear rates with the grinding effects of the rail surface material, such as White Etching Layer (WEL) and roughness. Although it was difficult to directly relate parameters, substantial information was acquired with regards to the mechanisms involved. Similar results were identified when comparing the rail samples from the laboratory and rails acquired directly from the field, proving that the methodology can simulate rail grinding successfully [5]. In this study the prime concentration was on moving towards the effects of different types of grinding process on the entire life-cycle of a rail material by initially grinding to simulate different maintenance schedules used in the field and then running the discs in a rolling-sliding test to represent train passage over the ground surfaces. Very little work has been done with regards to the grinding and post-grinding run-in effects on various rail grades [5,6]. As a result, part of the objectives of this project is to gain knowledge with regards to grinding in various premium materials under various scenarios. This will help understand if a relationship exists between the end-products of grinding (roughness, WEL) and hardness levels. The ground discs will be then subjected to post-grinding loading cycles to study the post-grinding effect on rail life-cycle. The post-grinding testing parameters employed for the "Normal usage" loading cycles aimed to understand the fatigue behaviour of premium hardened rail material in contrast to standard grade rail. Details for the experimental parameters utilised are presented in the following section 2.1. The term "Normal usage" was employed as the purpose of the post-grinding testing was to explore the effect of cycling loading. Hence the number of the cycles selected for the testing configuration as well as the loading parameters or conditions was set-up with the examination of post-grinding effects as the main objective. Moreover, the experimental parameters were directly adopted from a study by Santa et al. [7] that aimed to understand the fatigue behaviour of premium hardened rail material in contrast to standard grade rail. Fig. 1 describes the workflow of the study.

1.3. The scope

The aims of the study were to examine the grinding process thoroughly and understand its effectiveness under various conditions and scenarios. This was done by assessing preventive and corrective

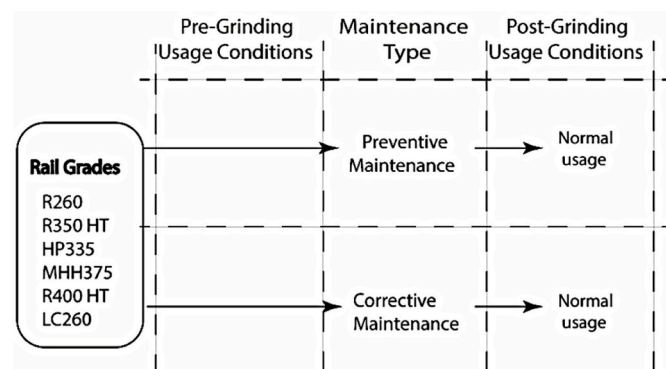


Fig. 1. Work process of testing.

maintenance processes on premium and standard rail grade materials. This allowed further knowledge to be acquired with regards to the effect of each maintenance type on the life cycle of various rail grades. Twin disc testing was carried out after the grinding process to evaluate the run-in performance of each rail grade.

2. Methodology and experimental procedure

As mentioned previously, the aim of the testing is to carry out a variety of experiments to assess the impact of grinding maintenance types on various rail grades and study the post-grinding effect on rail life-cycle.

2.1. Test rigs

The test rig was designed and manufactured by the Grupo de Tribología y Superficies at the Universidad Nacional de Colombia. The same equipment was utilised for a previous work [1].

Fig. 2 shows a schematic of the test-rig. The grinding wheel is coupled to a motor that can run at a fixed speed of 3600 rpm. This rotational speed of the grinding wheel is identical to what is utilised in the field. The whole grinding wheel-motor structure is placed on a linear roller bearing to allow sliding movement of the grinding stone towards the rail disc to enable grinding of the disc surface. The grinding wheel was acquired directly from the field and has identical specifications to the ones used in rail grinding. It is resin bonded Al₂O₃ and the dimensions comply with US standards of 8 inches in diameter

The rail specimens used were machined out of real rail steel to have material properties comparable to the real-world. Dimensions of rail discs are of 10 mm width and 47 mm diameter. A representation of the specimen cutting position in respect to the rail and the ground surface of the specimen is presented in Fig. 3. The grinding force applied onto the rail disc is monitored via a load cell and controlled by adjusting the position of the grinding wheel axis. It should be stated that the energy and mechanics of the small-scale grinding testing experiments performed in laboratory are not directly representative to the processes occurring in the field, however similar patterns [5] were aimed to be adopted.

To examine the grinding efficiency of conventional grinding, several experiments were performed with two main scenarios, preventive and corrective. A summary of the conditions utilised is shown in Table 1. For the preventive maintenance testing, a similar methodology to a previous study was followed [1]. As soon as the grinding wheel and rail discs reached their required speed the grinding wheel moved towards the rail specimen. The grinding time started when the first sparks appeared. After the first contact a 5 kg load was maintained for 30 s. This allowed comparable material to be removed considering the preventive grinding processes existing in the field over a similar number of grinding passes [5,8]. The rail specimens were then removed for measurements to be taken on the material removed in terms of mass loss and radius reduction. This procedure indicated the completion of one pass. Multiple passes were done to reach an overall 0.25 mm removal depth from the radius of the disc. Similar to the preventive maintenance experiments, the corrective maintenance experiments started when the grinding wheel made the first contact with the rail disc and sparks appeared. For this experiment a load of 60 kg was applied during the testing for 90 s. This allowed removal of a significant amount of material in a very short time period, similar to a corrective maintenance approach. The rail discs were then removed to determine the total material that was removed in terms of mass and radius.

For all the experiments a rolling/sliding test was performed after the grinding experiments to simulate the cyclic loading experienced by wheel and rail in the field and generate wear on the discs imitating the field conditions. For this experiment the SUROS twin disc test-rig was used to simulate the rolling/sliding between rail and wheel. This method has been used in previous studies [9,10]. A schematic of the test rig is

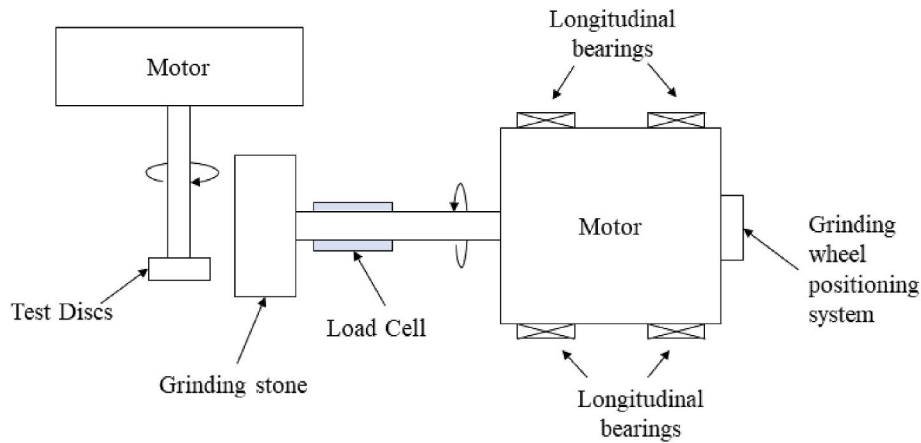


Fig. 2. Schematic representation of the equipment used for the grinding experiments [4].

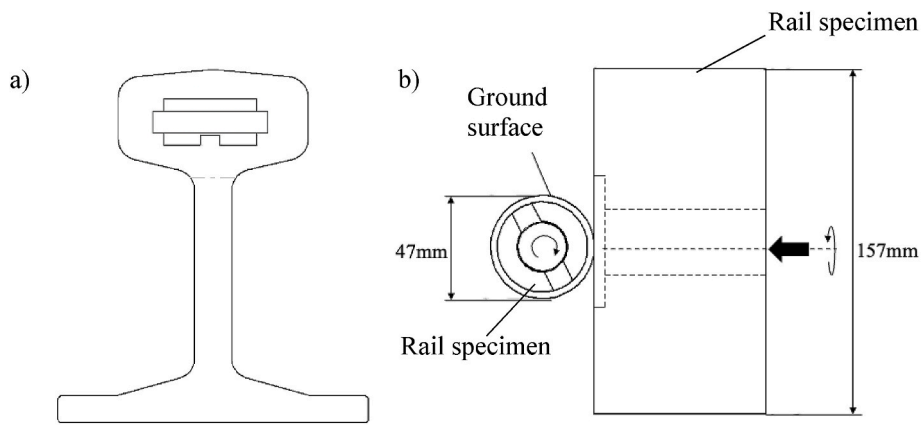


Fig. 3. Representation a) Disc specimen cutting position and b) ground surface on the specimen.

Table 1

Testing parameters for multiple passes experiments.

Maintenance type	Grinding Wheel Speed (Vs -rpm)	Specimen Speed (Vw -rpm)	Applied Load per pass (N)	Overall Grinding Time per pass(es)	Number of passes
Preventive	3600	700	49.05	30	>5
Corrective	3600	700	588.6	90	1

presented in Fig. 4. During the testing the torque between discs was measured and used to calculate the tangential force. The tangential forces were used to determine the coefficient of friction of the contact area. The length of the contact zone is the width of the cylindrical sample (10 mm).

Following a study by Santa et al. [7] that aimed to understand the fatigue behaviour of premium hardened rail material in contrast to standard grade rail, similar testing parameters were adopted. The parameters employed included 8000 dry cycles under 1% slip ratio and a maximum contact pressure of 1300 MPa for assessing normal usage wear. According to Esveld et al. [11] a slip percentage of around 1% is a reasonable level of slip for trains operating under normal conditions. Regarding the contact pressure of a rail/wheel it ranges typically between 800 and 1500 MPa, depending on various factors such as the material and geometry of the wheel and rail, the speed and weight of the train, and the condition of the track. However, the amount of 1300 MPa was chosen as this is the amount that is typically seen in high-speed or heavy-haul railway systems [11]. The number of cycles was chosen as Santa et al. [7] showed that coefficient of friction is stabilised up to 8000

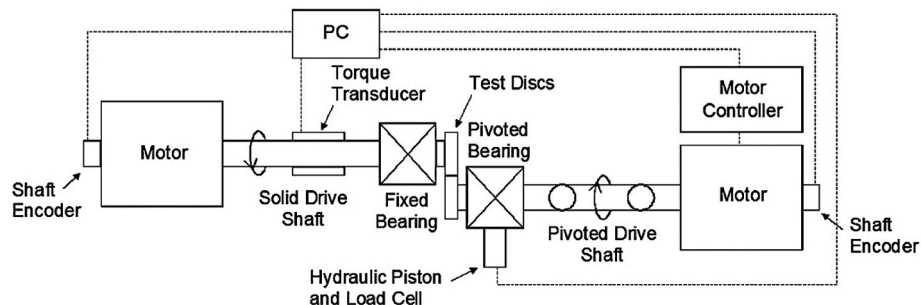


Fig. 4. Schematic of SUROS twin-disc machine.

cycles for various rail grades indicating its suitability for the purposes of this testing. It should be stated that the experiments performed were configured so as the effect of cyclic loading post grinding could be examined. Hence the number of the cycles selected for the testing configuration, as well as the loading parameters or conditions, were set-up with the examination of post-grinding effects as the main objective rather than the testing of the samples in the RCF or wear regimes. Thus, these tests should not be considered as RCF experiments of each rail grade, but only an indication based on the results obtained.

Throughout the test, the laboratory temperature was 25 °C, and relative humidity varied between 26% and 31%.

2.2. Materials

The rail specimens used in the grinding experiments were machined from rail grades of R260, HP335, R350HT, MHH375, R400HT, and Laser Clad R260 (LC 260). The R260 sample represent the standard rail grades while the rest of the samples are considered premium due to the thermal head-hardening and/or alloying processes they have been subjected to. All disc samples were extracted from rail sections. The LC 260 discs then underwent further processing by cladding layer of Martensitic Stainless Steel (MSS) of 1 mm on the disc surface which was then ground to achieve a similar surface finish to the unclad discs [12]. All the discs were machined to give a disc with contact width of 10 mm and a diameter of 47 mm. The wheel was machined from a BS5892-3 grade R8 wheel.

The chemical composition of rail grades as well as the wheel material is presented in Table 2 along with mechanical properties. Information regarding the hardness of each grade are presented in the following section.

2.3. Roughness measurements

Roughness measurements were taken in various instances. This was done in two ways:

- 1) Directly using an Alicona InfiniteFocusSL 3D measurement system with a 5X magnification lens and a cut-off wavelength of 800 μm to create a digital representation of the surface of the disc, and
- 2) Taking replicas of the disc topography by applying a layer of Microset 101 Thixotropic replicating compound to the disc's surfaces, adding a piece of backing paper, and waiting 6 min for the replica to set. The replicas were then similarly analysed using the Alicona system.

The development of surface roughness during the post-grinding

twin-disc testing was monitored after: 0, 200, 400, 600, 1000, 1400, 1800, 2200, 2600, 3000, 3400, 3800, 4500, 5500, 6500, 8000 test cycles. The methodology for monitoring the roughness at specific intervals was as adopted in previous studies [4,13]. In detail, the replica procedure followed was:

- Stopping the test and waiting for the discs to cool
- Cleaning the discs in an acetone bath
- Applying a layer of Microset 101 Thixotropic replicating compound to the disc's surfaces, adding a piece of backing paper, and waiting 6 min for the replica to set
- Using an Alicona InfiniteFocusSL 3D measurement system with a 5X magnification lens and a cut-off wavelength of 800 μm to create a digital representation of the surface of the replica
- Choosing lines with a minimum length of 4 mm on the digital image along which the Alicona software calculated roughness measures
- Cleaning the discs in an acetone bath
- Mounting the discs to continue the experiment

2.4. Microstructure analysis

After the twin-disc tests, the discs were sectioned, polished and then etched in 2% Nital to allow examination of the microstructure and any cracks present. The sectioned discs were assessed using both optical and scanning electron microscopy.

3. Results

In this section the results from the all the test groups are presented. Sectioning of the specimens was done in the cross-sectional direction defined as perpendicular to the rolling direction. The roughness measurements of the discs at various instances are also presented. It needs to be noted that the roughness on the longitudinal direction was only considered as there is no slip in the lateral direction. Due to the large number of specimens, a representative figure from each group is shown.

Data are split into three subsections: **Preventive Maintenance**, **Corrective Maintenance** and **Post-Grinding Performance**. Post-grinding performance exhibits the results that were collected to examine the run-in performance of the disc after grinding to examine the effect of roughness and material phase change.

The discs from each rail grade were examined to specify their pre-test hardness levels for future consideration in the data comparison. Hardness data are presented in Fig. 5. The rail grade exhibiting the lowest hardness level is the 260 with the hardest grade being the LC 260. Due to material unavailability, R400 HT was not tested in a post-grinding performance experiment.

Table 2
Chemical composition (wt%) and mechanical properties of the various rail grades and wheel material used in testing.

	C	Si	Mn	P	S	Cr	Al	V	Cu	Ti	Ni	Mo	Co	W
R260	0.736	0.270	1.056	0.032	0.023	0.026	-	0.003	0.002	0.016	0.021	0.006		
HP 335	0.87-0.97	0.75-1	0.75-1	≤0.02	0.008-0.020	≤0.10	≤0.004	0.09-0.13	-	-	-	-		
R350 HT	0.736	0.270	1.056	0.032	0.023	0.026	-	0.003	0.002	0.016	0.021	0.006		
MHH 375	0.72	0.40	0.8	≤0.02	≤0.02	0.4	≤0.004	≤0.03	-	-	-	-		
R400 HT	0.931	0.251	1.269	0.009	0.022	0.275	-	0.0035	0.017	0.002	0.015	0.0068		
LC 260	0.22	0.18	0.87	0.011	<0.003	9.53		0.27	<0.01		2.25	0.24	1.22	0.46
E8	0.542	0.253	0.734	0.011	0.06	0.141	0.027	0.006	0.165	0.002	0.120	0.048		
Tensile Strength (MPa)														
R260														≥880
HP 335														≥1150
R350 HT														≥1175
MHH 375														≥1280
R400 HT														≥1280
LC 260														≥1379
E8														860-980

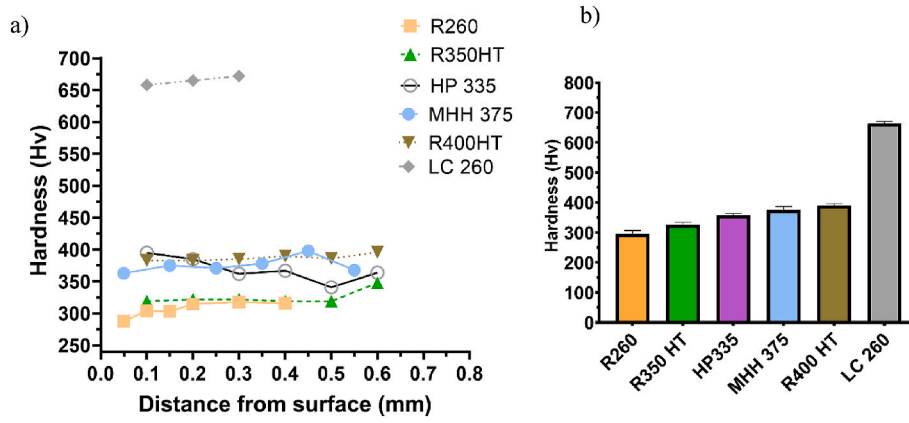


Fig. 5. a) Hardness testing on the various rail grades; b) Average hardness values for each rail grade.

3.1. Preventive maintenance

Each rail material needed a different number of grinding passes to achieve the required depth of cut. Thus, the rate of material loss for each rail grade is presented in Fig. 6. Each grinding pass was converted to metres to project the distance over which the grinding stone stayed engaged with the rail disc. The mass loss per distance rate differs for the various grades due to the fact that discs comprise dissimilar microstructure and hence have dissimilar resistance to the material removal process. As expected, the 260 grade, which has the lowest hardness, exhibits the highest material loss (μg)/distance (m) parameter that translates into the lowest resistance to the material removal process. On the other hand, the LC 260 which exhibits significantly higher levels of hardness demonstrates the lowest level of material loss/distance ($\mu\text{g}/\text{m}$). Fig. 6 also presents the roughness data obtained from the freshly ground surface of the discs. The roughness of the discs prior to the grinding experiments was $0.5 \pm 0.05 \mu\text{m}$ (Ra). Values of Ra and Rq are presented; the roughness values are comparable for the different materials, and it can be clearly observed that there is a trend with all the Ra and Rq values being between 3.5 and 7 μm . The only variation from the trend is observed on the laser clad disc which has a significantly higher hardness than all the other rail materials tested (see Fig. 5) and also showed a lower roughness after grinding.

Fig. 7 represents the images of the samples' microstructure taken with an optical microscope and SEM. The common observation in all the specimens apart from the LC 260 is the existence of WEL on the running surface. This is due to the fact that the laser clad material does not

undergo a martensitic phase transformation under excessive plastic deformation or rapid cooling from high temperatures (above 700 °C). Furthermore, the WEL observed in the other specimens can be characterised as discontinuous. Additionally, the inclusions detected within WEL in Fig. 7 could act as crack initiators in the post-grinding run-in [14]. This indicates that the crucial parameters involved in the formation of WEL (plastic deformation and temperature) were not sufficient or they did not occur for an adequate time to create a uniform thickness. The variance of the WEL shape can be decisive in the post-grinding performance of the rail discs and the development of any defects. As determined in another study [5] discontinuous WEL can be delaminated more easily during the run-in process without affecting the performance of the rails and initiating any defects. The thickness of the WEL observed in the discs' microstructure are between 1 and 8 μm . Fig. 8 exhibits the WEL thickness detected on the various rail grades. As it can be seen, the maximum thickness is similar in all grades, however, the mean value is different indicating that the frequency the maximum thickness appeared at is different in each sample. The R260 exhibited the highest mean value with R350 HT demonstrating the lowest.

3.2. Corrective Maintenance.

In this set of experiments there was no control over the diameter reduction. A load of 60 kg was applied for a time period of 90 s. Fig. 9 shows the roughness and mass loss rate. For most of the disc specimens the losses were in excess of 15 $\mu\text{g}/\text{m}$. However, in rail discs with significantly higher hardness levels, like LC 260, the exhibited degree of material loss was smaller. Similar to the specimens utilised in the preventive maintenance, the roughness of the rail discs prior to the grinding

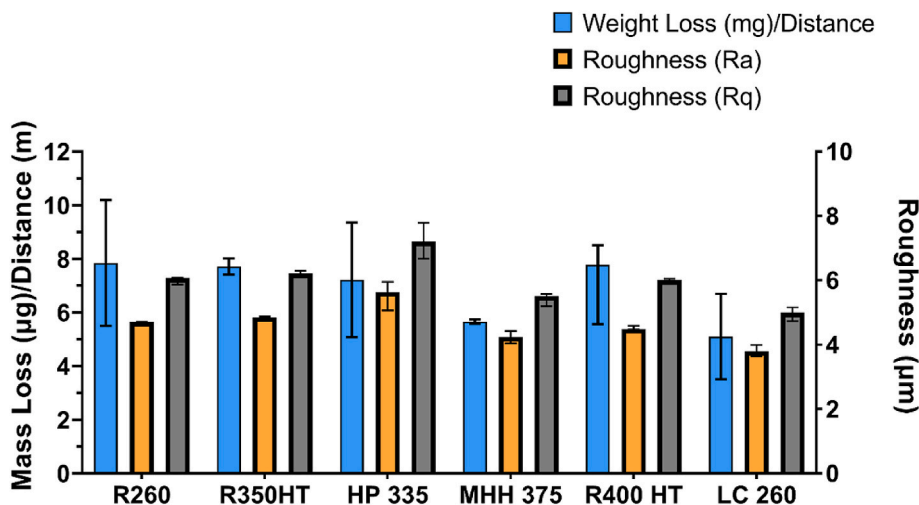


Fig. 6. Mass loss and roughness of discs ground with the preventive maintenance configuration.

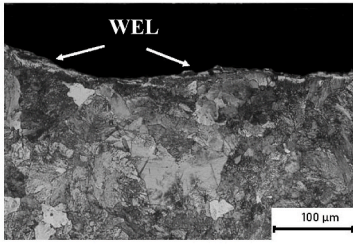
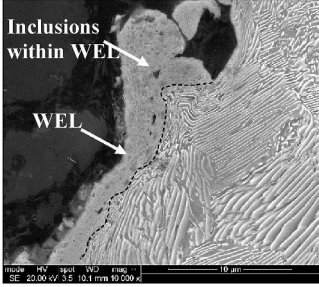
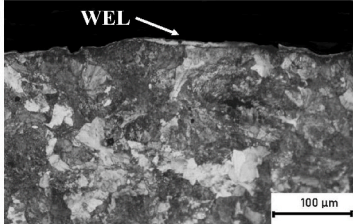
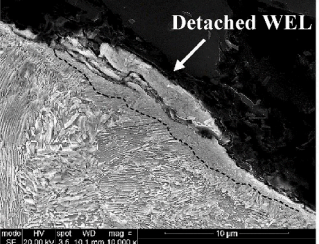
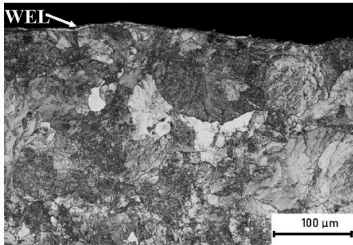
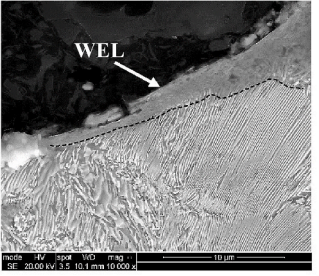
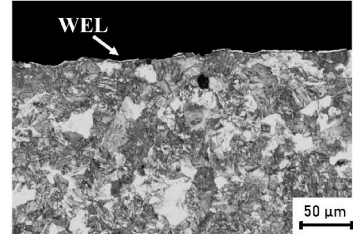
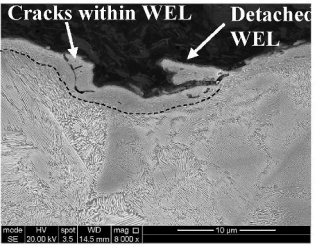
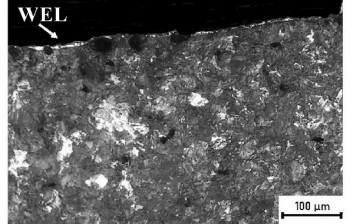
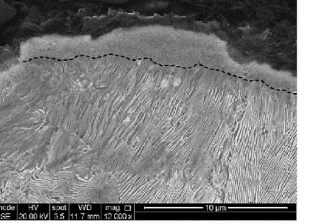
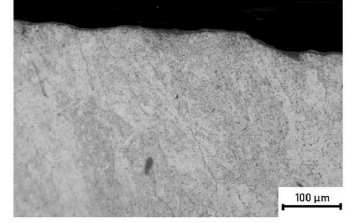
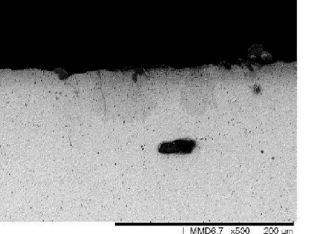
	Microscope Image	SEM image
R260		
R350HT		
HP 335		
MHH 375		
R400 HT		
LC 260		

Fig. 7. Microstructure analysis of the rail discs subjected to a preventive maintenance process.

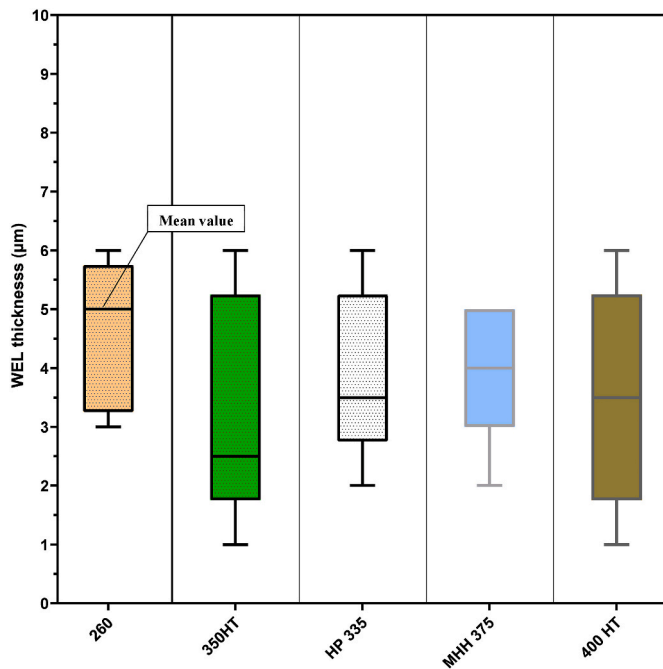


Fig. 8. WEL thickness comparison across the rail grades for the preventive maintenance grinding.

experiments was $0.5 \pm 0.05 \mu\text{m}$ (Ra). Fig. 9 also represents the roughness measurements of the rail discs. Most of the rail discs exhibit roughness (Ra) values in the region 4-5 μm . However, rail specimens with elevated hardness such as R260 MHH375 and LC 260 display roughness (Ra) below 4 in the range of 3.6–3.9 μm .

As done previously, to analyse the microstructure, the specimens were sectioned to acquire a cross sectioned view. As it can be clearly seen in Fig. 10, WEL exists in all the disc images similar to the preventive maintenance results. The WEL is located on top of the contact surface, which indicates material transformation during the grinding process. However, in comparison with Fig. 7 a thicker layer has been developed on most of the discs. In many cases it was found that the WEL is continuous along the running surface exhibiting lengths of at least 200 μm without interruptions. This is more noticeable in the MHH375 and R400 HT specimens where the WEL is thicker and more consistent along the surface. On the contrary in the preventive maintenance results, the corresponding images of MHH375 and R400 HT discs showed that the WEL is interrupted and thickness varies along the surface. The cracks

observed within the WEL in some of the images are very important and need to be considered to determine the effect they have on the life of the disc. Overall the physiology of the WEL will be taken into account in the post grinding performance experiments to determine whether a more uniform layer can affect differently the generation of cracks and defects. Following the microstructural analysis, a comparison of the thickness of WEL was done between the different rail grades. Fig. 11 displays the data collected regarding the WEL from all the materials. It was found that the mean value was similar in all grades however there was a significant increase compared to the thickness observed in the preventive maintenance scenario (see Fig. 8). This indicates the effect of the grinding parameters on the WEL formation.

3.2. Rail disc roughness

Due to the large amount of data collected during the experiments some representative comparisons were made to draw conclusions. For these purposes the R260 and MHH 375 specimens were utilised after they were ground in a preventive and corrective manner.

A comparison between two R260 grade discs is presented in Fig. 12 a). The two discs have been ground by the same stone. However, the methodology that was used included multiple passes for one disc and a single pass for the other disc. In terms of the material that was removed from the disc, in the corrective maintenance experiments a significantly larger amount of material was removed from the disc compared to the preventive maintenance experiment. Fig. 12 a) demonstrates almost 2.5 times more material was removed from a specimen ground using a corrective method with a 4.22% weight reduction compared to 1.56% weight reduction of the preventive maintenance specimen. The roughness values on the two discs are 4.24 μm and 4.56 μm respectively. Regardless of the material that has been removed the roughness measurements are very similar in both cases verifying that the main factor affecting the surface topography is the grinding stone. Similar, to the previous comparison, data was collected from two MHH 375 grade discs and is presented in Fig. 12 b). The two discs have been ground by the same stone. However, the methodology that was used included multiple passes for one disc and a single pass for the other disc. As it can be seen on Fig. 12 b) the amount of material removed from both discs is slightly larger on the multiple passes test with 1.72% weight reduction compared to the 1.10% reduction on the single pass test. Regarding the roughness of matching rail grades from the multiple pass experiments and the single pass experiments, they exhibit similar roughness values. This is demonstrated in Fig. 12 through the data collected from the R260 and MHH 375 discs following the corrective and preventive maintenance processes. The roughness levels of each grade in the respective

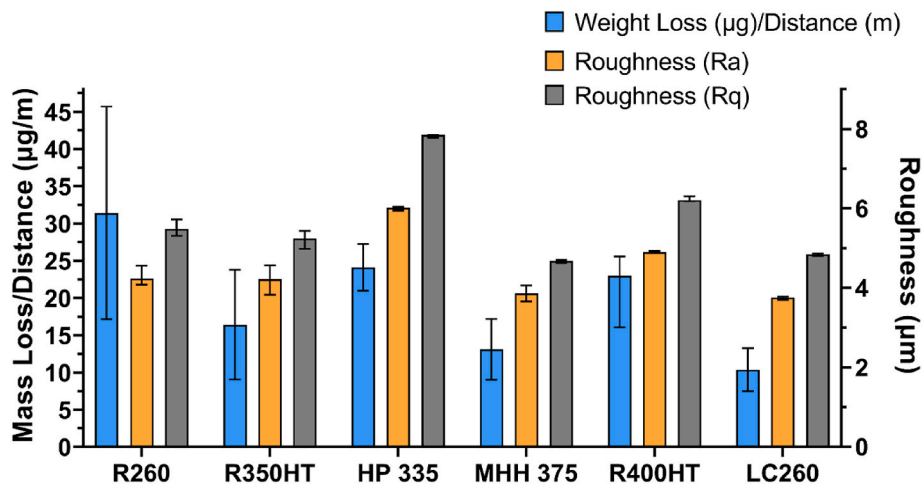


Fig. 9. Roughness comparison between all the different rail discs for single pass grinding experiments.

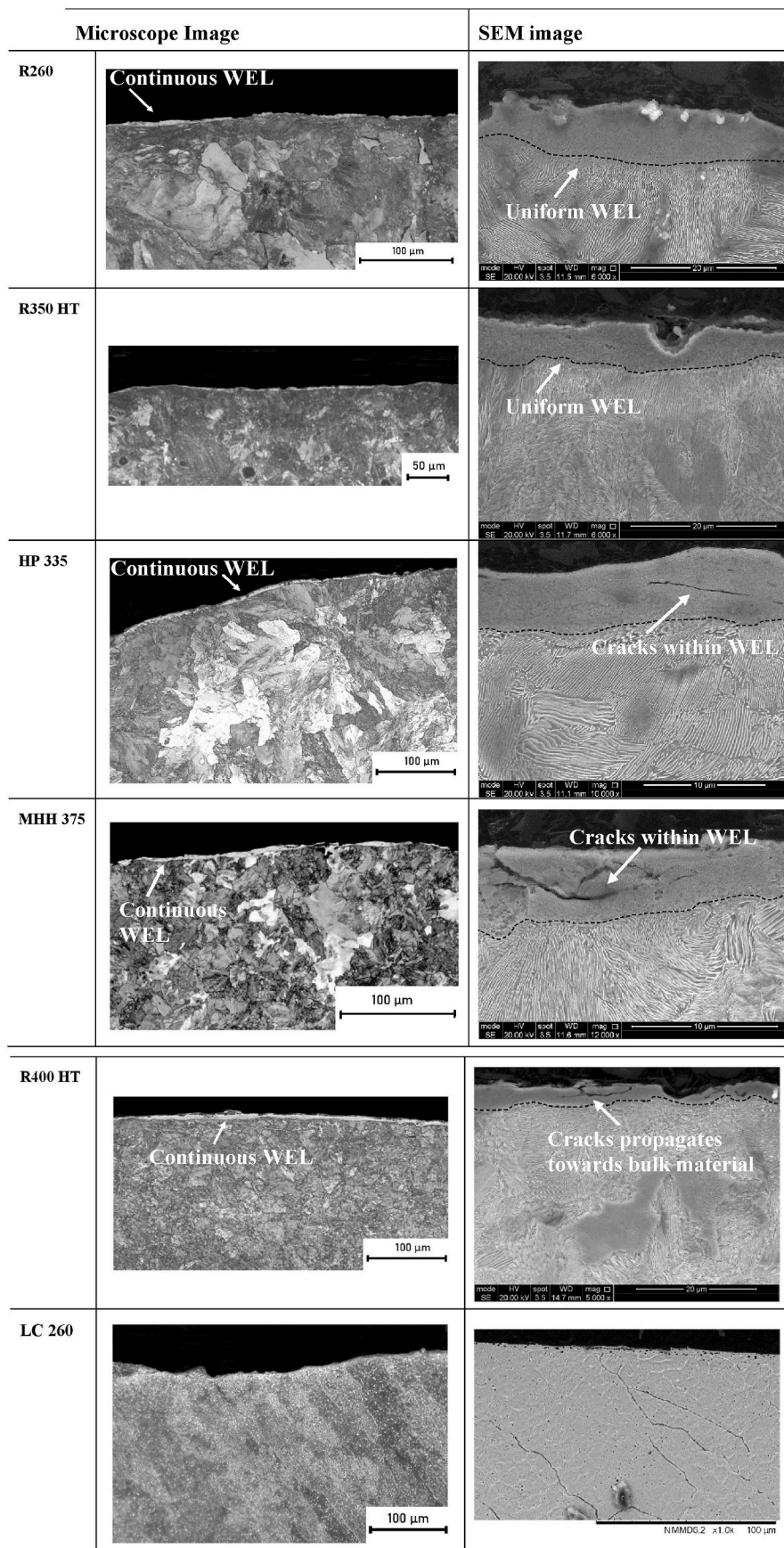


Fig. 10. Microstructure analysis of the rail discs subjected to a corrective maintenance process.

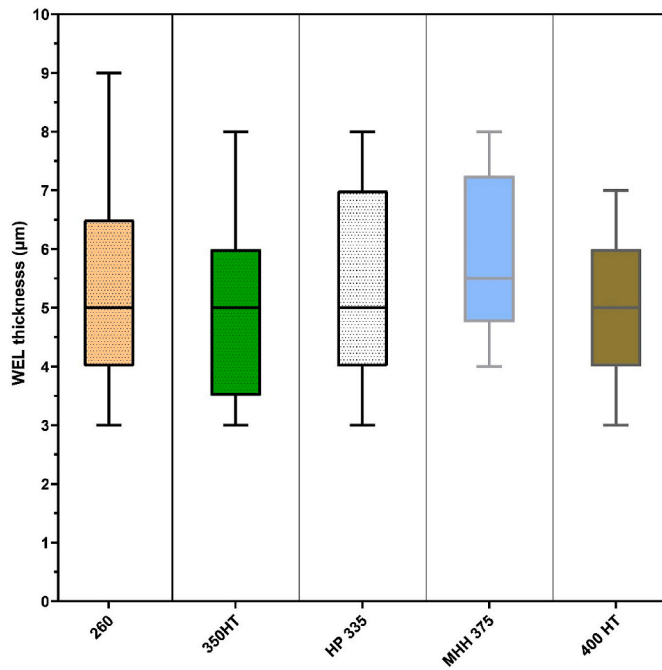


Fig. 11. WEL thickness comparison across the rail grades for the corrective maintenance process.

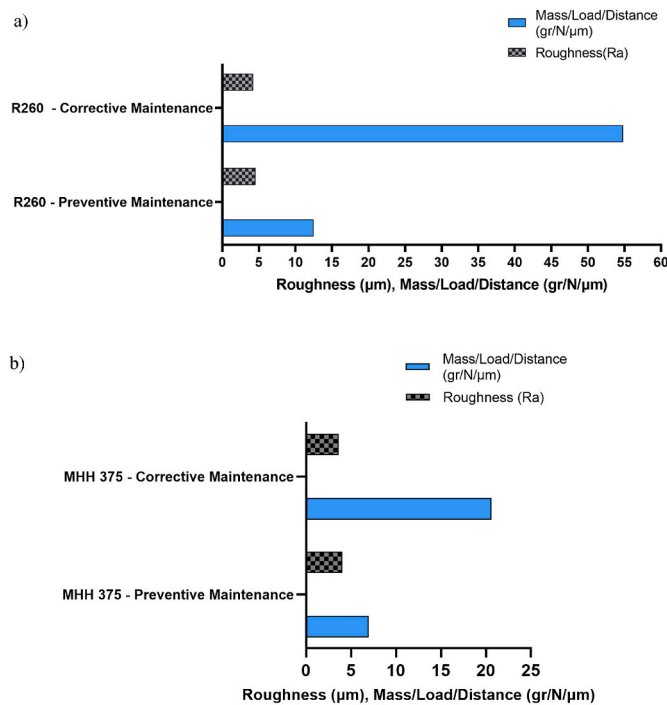


Fig. 12. Representation of the mass loss and roughness data collected from a) R260 rail discs following the corrective and preventive grinding experiments; b) from MHH375 rail discs for corrective and preventive grinding processes.

maintenance processes are alike. Hence, it can be clearly concluded that the maintenance process does not affect the final surface topography of the specimen. Furthermore, comparing both rail grade’s roughness from Fig. 12, it can be said the two grades exhibit similar values of roughness (around 4.5 µm), thus the resulting roughness from a grinding process is entirely based on the grinding wheel topography.

3.3. Post-grinding performance

As described in Section 2, all the discs materials were run for 8000 cycles. The discs were tested in a rolling/sliding regime to imitate the conditions a wheel and rail are subjected to after the occurrence of grinding. A point of interest in this study is to determine whether the WEL still exists after the twin-disc testing process or whether it is delaminated and whether any other damage has been initiated or propagated.

3.3.1. Preventive grinding

The friction data obtained from the post-grinding twin-disc testing are presented in Fig. 13 a). As expected, the specimens underwent a run-in stage where the coefficient of friction between the rolling surfaces experienced a gradual rise. This stage took place between 0 and 2000 cycles with some specimens going through this phase quicker, such as R260, and other specimens taking more time, such as MHH 375. This process occurs as on a micro-level during the initial run-in where the asperities formed due to grinding are smoothed out from the shear forces and normal load applied on the discs. As the experiment continued the coefficient of friction slowly stabilised around a value of 0.4 at 8000 cycles. The smoothing of the asperities is visually represented in Fig. 13 b) via the roughness data that were collected throughout the experiments. It can be seen that the R260, R350 HT and MHH 375 specimens exhibit similar behaviour with the final roughness values being increased after an initial decrease due possibly to cracks being generated, affecting the roughness values. Also, the delamination of WEL will contribute to the increase of the roughness. Others such as the HP 335 and LC 260 demonstrate a constant decrease of roughness without

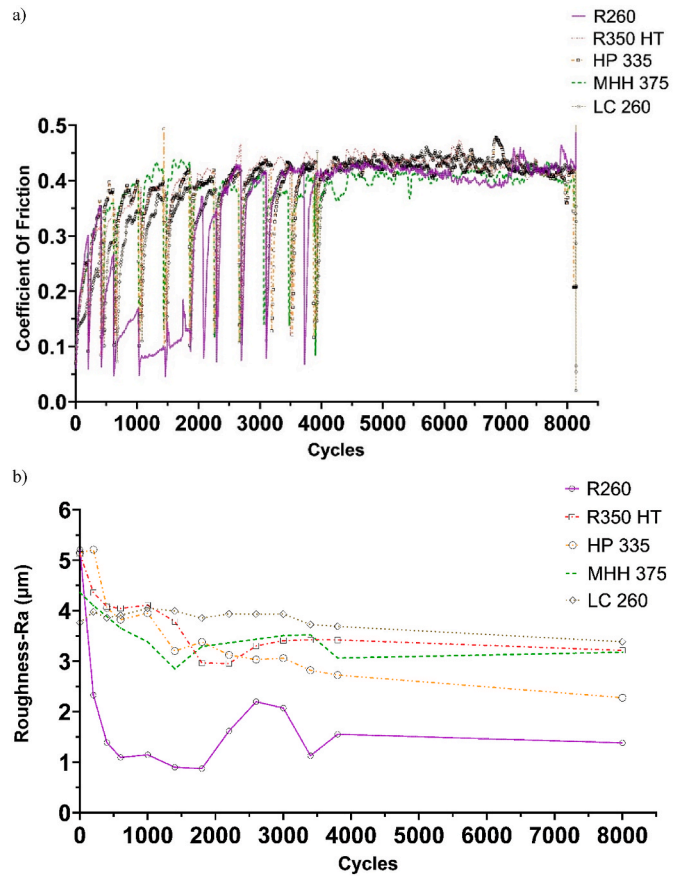


Fig. 13. Data obtained during the post-grinding twin-disc testing of the specimens that underwent a preventive maintenance process: a) the coefficient of friction and b) roughness.

reaching a stable value. As these are harder rail grades, a different mechanism is expected to occur during the smoothing of the asperities. Additionally, LC260 exhibited no material transformation on the running surface, hence no delamination would affect its roughness development.

Fig. 14 illustrates the wear rates of the discs that were ground following a preventive method and further tested in rolling/sliding experiments. The results are in agreement with the expected trend as the harder rail materials were expected to demonstrate less deformation and wear compared to the less hard rail grades. The LC 260 demonstrates the lowest wear rate and R260 the highest. The rest of the rail grades fall in between.

The specimens assessed in the twin-disc testing were sectioned for further analysis on a microstructural level. The preparation of the specimens was done as detailed in Section 2.4. Fig. 15 represents the microstructure of the R260 specimen that was previously ground in a preventive manner. A deformed layer can be clearly seen on the top running surface of the disc indicating the significant amount of shear forces it experienced that resulted in the deformation of its pearlitic structure. Near the top running surface, it can also be seen that some WEL remained. The normal and shear forces applied to running surface during the twin-disc testing resulted in the crushing and delamination from the bulk material of the majority of the WEL presented in Fig. 7. As a result, only some small bits of WEL are present after the completion of the experiments. A similar phenomenon was observed by Zhou et al. [15] on comparable disc specimens where the WEL delamination occurred during a twin-disc rolling/sliding experiments. Furthermore, findings from that study indicated that the delamination of WEL can result in the formation of squat-type defects.

Further images were taken on all the grades utilising the optical microscope and SEM. The amount of WEL remaining is significantly larger compared to the R260 in Fig. 15. Furthermore, it can be said that the WEL remaining on these grades are embedded into the pearlite structure below the running surface. As the images indicate the deformation of the material resulted in the pearlite fully overlaying some of the remaining WEL and pushing it further towards the bulk material. SEM images were taken with particular focus on the remaining WEL. As it can be observed in the SEM images of Fig. 16 cracks exist near the WEL indicating its effect on the microstructure of the discs. The HP335 images showcase two clear cases where the brittle nature of the WEL resulted in crack formation within the martensite layer and the propagation or branching of cracks towards the bulk material. Although the MHH 375 does not demonstrate a similar case, some cracks are present

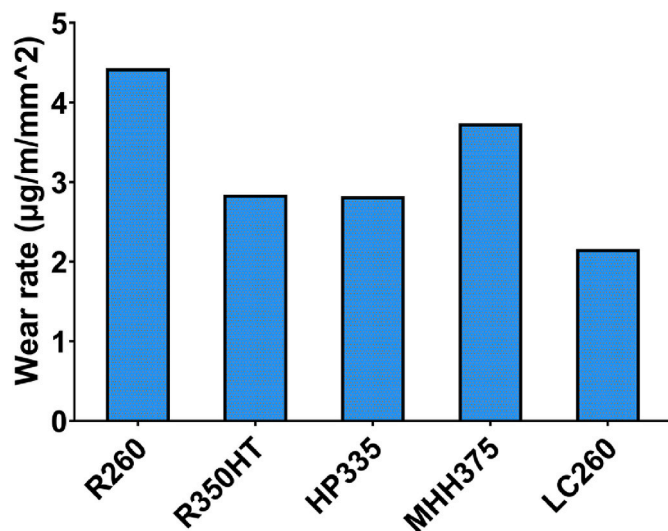


Fig. 14. Rail disc wear rates that were previously ground in a preventive method.

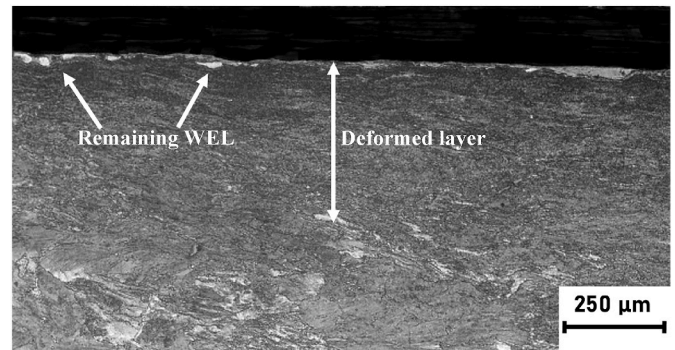


Fig. 15. Microstructural analysis of R260 specimen after the run-in experiments (8000 cycles).

in an overlaid WEL that with further usage of the discs could potentially spread in the pearlitic structure. Furthermore, the SEM image of the MHH 375 displays large amounts of overlaid WEL still present subsequently to the twin-disc testing. As demonstrated, this can result in the crack formation near the point of WEL as the large quantities of martensite cannot be fully covered by pearlite causing the separation of pearlite layers.

Fig. 17 demonstrates the continuous bands of martensite that remained as well as the deformation layer on each rail material upon completion of the twin-disc testing. Results present short continuous WEL lengths in R260 and longer martensite bands in the harder materials with HP 335 exhibiting the longer continuous WEL. As expected, the deformed layer below the WEL is smaller on the harder materials.

3.3.2. Corrective grinding

The performance of the discs that underwent a corrective maintenance process was also studied with the aid of rolling/sliding tests. Results from the experiments are presented in Fig. 18. The coefficient of friction follows a similar trend to the previous specimens with a sudden increase at the beginning followed by a decrease and eventually its stabilisation. However, in most specimens it is observed that the initial stage of run-in extends up to 3000 cycles. Furthermore, during the initial run-in in most specimens it was observed that the coefficient of friction is slightly higher compared to the previous results shown in Fig. 13; nevertheless, the coefficient of friction is again stabilised around 0.4 at 8000 cycles. Regarding the roughness, the results demonstrate a trend similar to the previous experiments, i.e., the initial, rough surfaces from the grinding process are gradually smoothed due to the shear forces of the rolling/sliding mechanism and the normal load applied between the two running surfaces. The surfaces reach a steady-state that is followed by a short increase due to the transition into the wear stage. However, this trend is not followed by HP 335 and LC 260 specimens. The LC 260 keeps a constant value of roughness that fluctuates around 4.5 µm and the HP 335 specimen showed a continuous decrease throughout the experiments.

The wear rates of the correctively ground discs that were further tested in rolling/sliding experiments are presented in Fig. 19. The results from the preventive maintenance experiments were also added for comparison purposes. The wear rate of LC 260 is significantly lower than the rest of the specimens as the hardness of the disc is higher than the rest, thus it is more resistant to wear. The behaviour exhibited can be associated mostly with the hardness of the rail materials as the R260 exhibits the highest wear rates in comparison with the corresponding wear rates from the preventive and corrective maintenance experiments of the rest of the rail grades. With regards to the corrective maintenance results the MHH 375 showcases the lowest wear rates with the R350 HT and HP 335 in between them. The increased amount of wear of R260 from the corrective maintenance experiments could be due to the large amount of WEL being delaminated throughout the testing on top of the

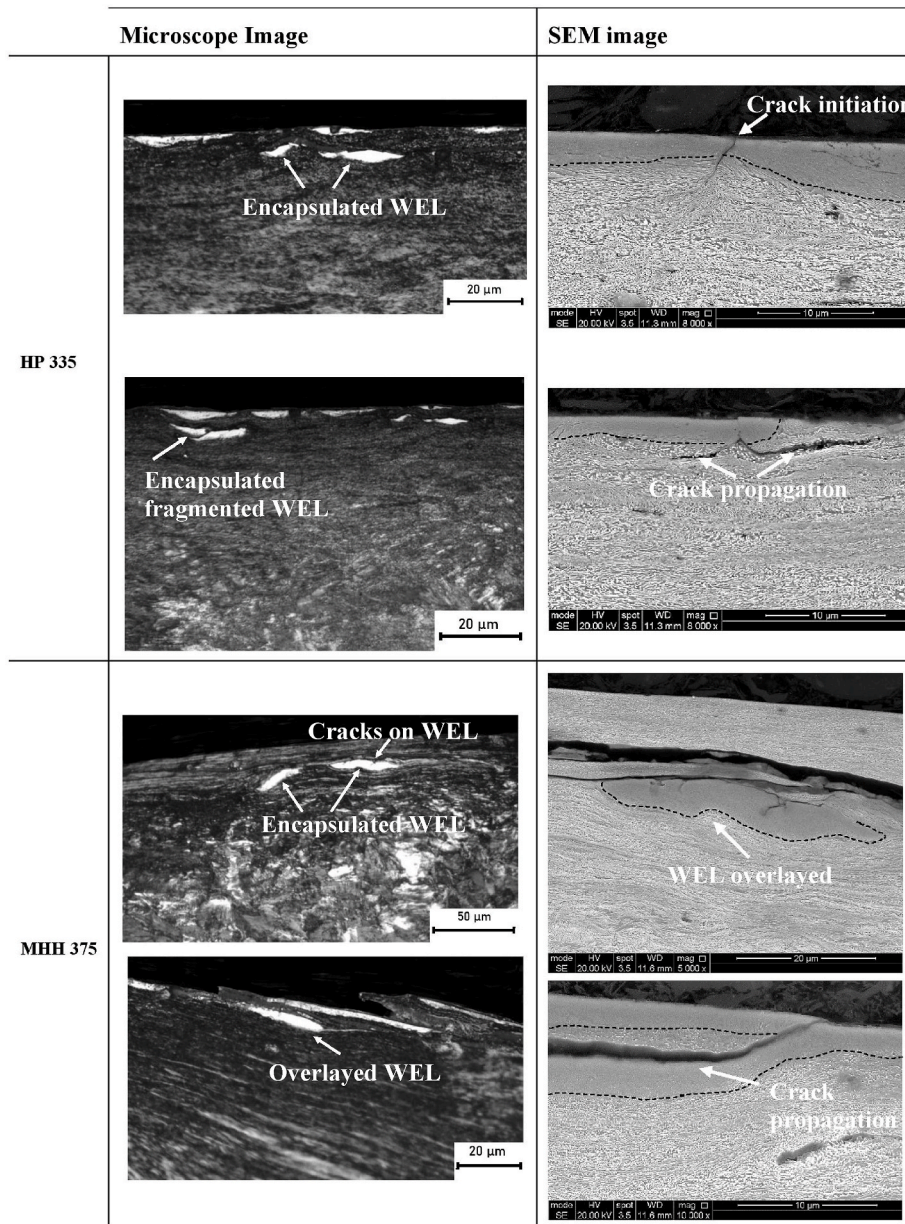


Fig. 16. Optical and SEM images of the rail specimen microstructures after the twin-disc testing.

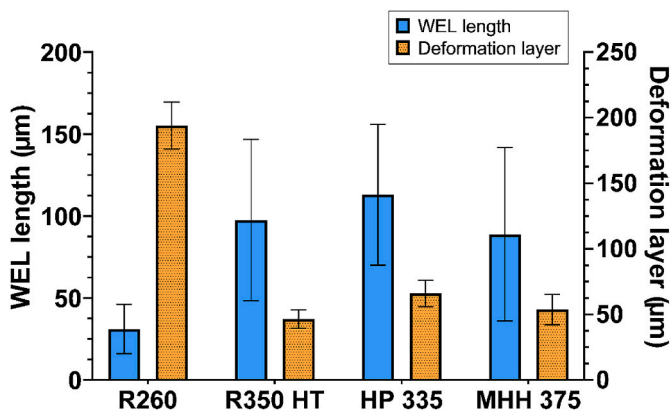


Fig. 17. Comparison of the continuous WEL length and deformation layer of each rail material ground under preventive maintenance.

normal wear the disc was subjected to.

As indicated earlier all the specimens subjected to a twin-disc testing were sectioned to further study their microstructure. Fig. 20 exhibits the microstructure of the R260 specimen. Through a direct comparison with the image in Fig. 15 it is clear that larger amounts of WEL remained after the twin-disc testing. This could be due to the fact that the initial amount of WEL presented on the specimen was larger as demonstrated in Fig. 10. Hence only part of the martensite layer can be detached through the rolling/sliding mechanism resulting in considerable amounts of WEL that could affect the performance of the specimen.

Due to time and space limitations only the HP 335, R350HT and MHH 375 grades were focused upon. Fig. 21 illustrates images taken utilising an optical microscope and an SEM. A direct comparison between the R260, the HP 335, R350HT and the MHH 375 suggest that the latter three showcase larger amounts of WEL. Due to the thicker WEL, numerous cracks were formed within the martensitic layer which are visible through the lower magnification of the optical microscope indicating their severity. Hence it can be said that the thickness of WEL in

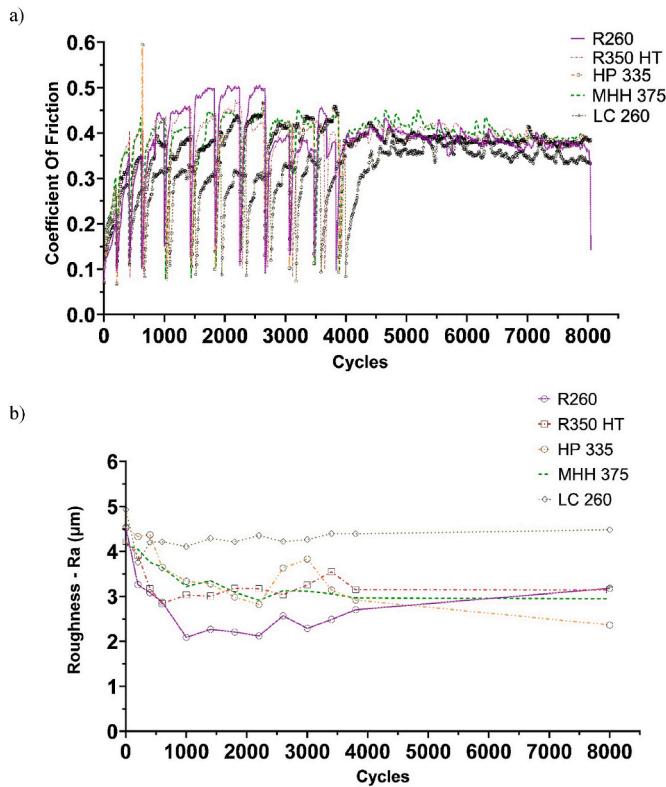


Fig. 18. Data obtained from the post-grinding experiments of the specimens that underwent a corrective maintenance process: a) the coefficient of friction and b) roughness.

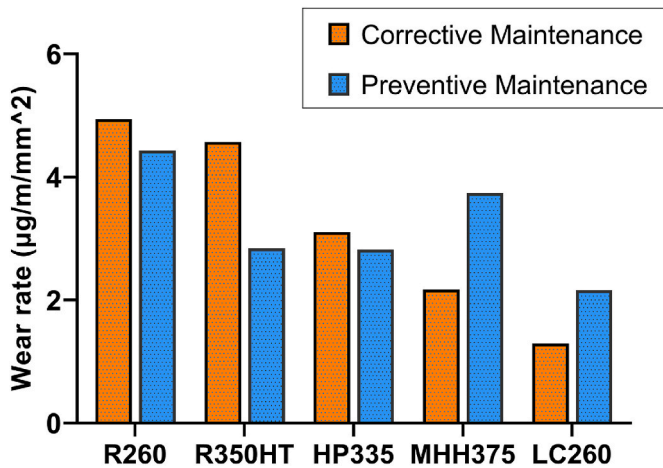


Fig. 19. Demonstration of the twin-disc wear rates using rail discs that were previously correctively ground.

the specimens that went through a corrective maintenance procedure has a significant impact on the formation of defects such as cracks. The SEM images from both specimens confirm the previously mentioned hypothesis as they display areas where cracks were formed, due to the brittle WEL layer, and propagated towards the bulk material. Additionally, the SEM image of the HP 335 demonstrates an instance where multiple cracks within the WEL meet while spreading, resulting in the detachment of a small piece.

Data regarding the continuous bands of WEL and the deformation layer that was observed in each rail material is presented in Fig. 22. Similar to the data presented in Fig. 17 the softer material exhibits the shorter continuous bands of WEL and the largest deformed layer from

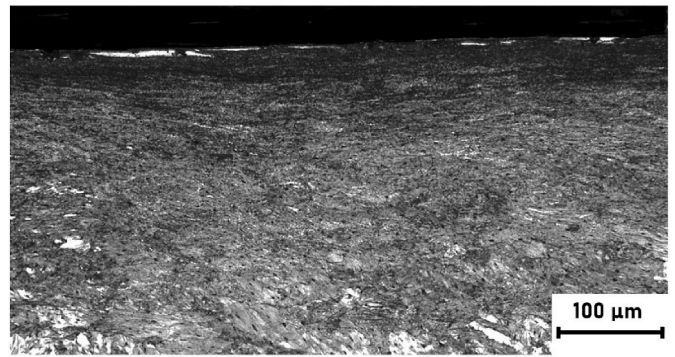


Fig. 20. Microstructural analysis of the R260 specimen that underwent corrective maintenance and then twin-disc testing.

the rolling/sliding testing. The data regarding the deformed layer is in agreement with the hardness data presented in Fig. 5 as the harder materials show more resistance to plastic deformation. Furthermore, the premium rails exhibit significantly longer continuous WEL compared to R260. As expected, the deformed layer below the WEL is smaller on the harder materials.

4. Discussion

An interesting observation made from the results in Section 3.4 is the variation of WEL quantities remaining on the rail grades upon completion of the experiments. It can be clearly stated that the harder materials tend to sustain greater quantities of WEL after being subjected to rolling/sliding cycles. This indicated an increased number of cracks and with some cases showing more severe cracks. An explanation of this phenomenon would be to consider the martensite layer as a hard coating on the steel substrate. The main cause of wear in hard coatings is the formation of microcracks that result in the spalling of the superficial layer. Hard coatings are divided into two main categories the thin coatings which are smaller than 1 µm as stated in the literature and the thick coatings are categorised as anything above 10 µm. The WEL formed on top of the discs lies in-between the two main groups, but it can be said that it is closer to the thick coatings. The substrate influence can result in the collapse and failure of the coating under high loading conditions due to the elastic and plastic deformation occurring. In contrast thick coatings can be more susceptible to low adhesion to the substrate due to the reduction of internal residual stresses in the film [16]. In both cases, to reduce the possibility of damage or cracking of the brittle coating, the substrate is hardened to minimise the plastic deformation of the subsurface and achieve a good hardness gradient at the coating-substrate interface. This would ensure a uniform strain distribution along the coating-substrate interface reducing the possibility of damage or cracking of the brittle coating [17]. In other cases, an intermediate hard layer is introduced between the hard coating and the substrate to reduce the hardness variation by absorbing the effect of the compressive stresses [18,19]. In the specimens tested under rolling/sliding conditions the hardness gradient of the WEL-pearlite interface varies with the rail grades. The harder grades such better support the hard and brittle layer reducing the stresses between the coating-substrate interface. However, in the case of the R260 where the bulk material is significantly less hard and more flexible, WEL fractures and collapses due to the combination of elastic and plastic deformation and consequently the increased stresses between the “coating” and “substrate”. This mechanism is illustrated in Fig. 23 with two possible resulting scenarios based on the results observed in Section 3.4: 1) the WEL remains attached to the bulk material and it is pressed into the pearlitic microstructure increasing the possibilities for crack formation due to this; 2) failure of the bonding between the WEL and the pearlite led to the complete delamination of the martensite layer. This

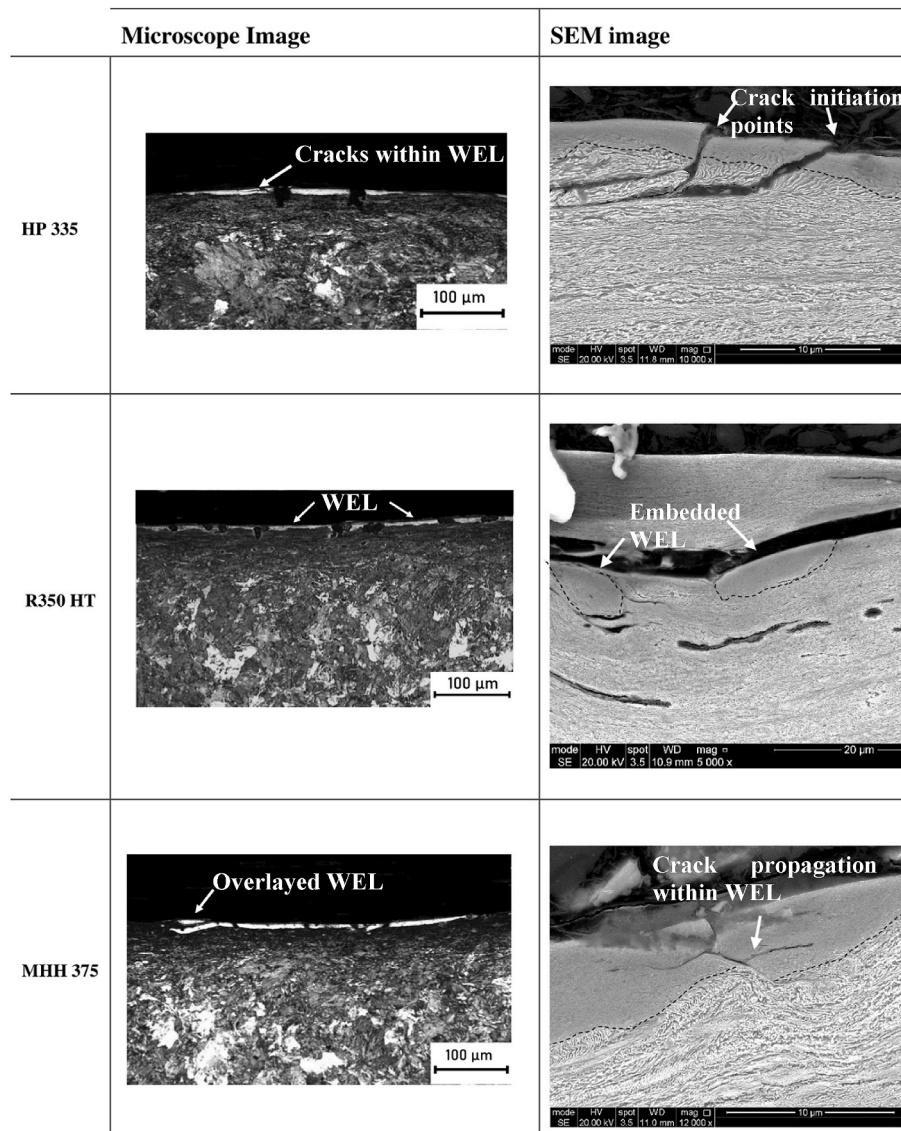


Fig. 21. Optical and SEM images of the rail specimen microstructure after the twin-disc testing.

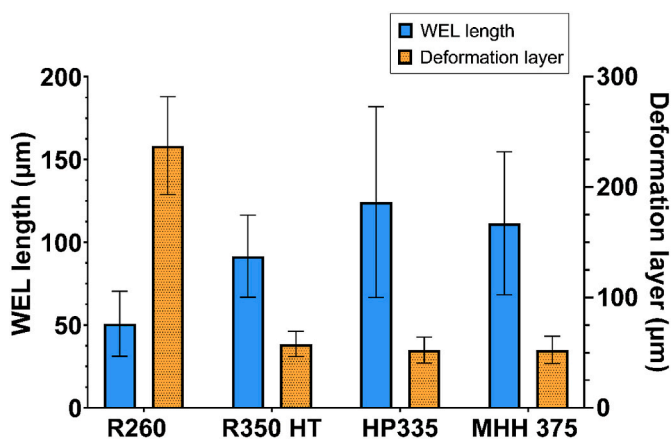


Fig. 22. Comparison of the continuous WEL length and deformation layer of each rail material ground in a corrective approach.

speculation is supported by the results presented in Fig. 16 and Fig. 21 where the harder rail grades showcase higher resistance to deformation reducing the probability of WEL fracture during the rolling/sliding mechanism, hence increasing the likelihood for crack initiation from the WEL due to its brittle nature. Furthermore, it was observed that the resulting microstructure in harder rails exhibited larger amounts of WEL upon completion of the run-in testing where in some cases they were overlaid and, in combination with their less ductile microstructure, more defects could be formed due to easier crack propagation. Thus, while the softer rail grades are expected to deform more, the absence of WEL from the early delamination during the run-in does not result in many overlay cases. Particular emphasis should be given to the fact that these are observation based on the results obtained. Further experiments are required to thoroughly examine this idea and verify it.

It was shown in Section 3 that both grinding processes had a similar effect on the microstructure. A phase transition occurred in most cases (apart from the LC 260 specimens) causing the formation of WEL on the grinding contact zone of the rail specimen. In the current experiment the mechanism that would be most appropriate to explain the transformation is the high temperature generated on the contact zone due to the frictional losses. The excessive heat combined with the material dislocation that took place resulted in the phase transition of pearlite i.

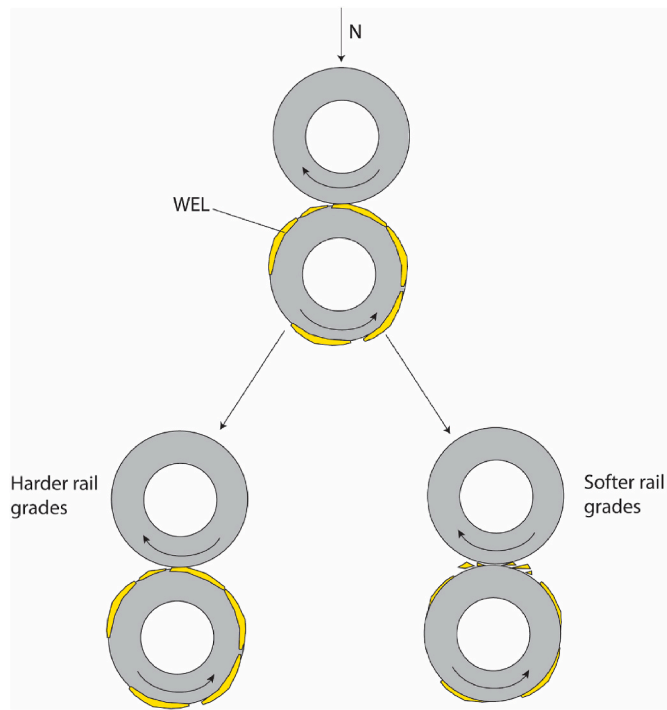


Fig. 23. Illustration of the WEL delamination of discs on dissimilar grades.

e., the formation of a martensite layer.

For the most part it has been noticed in Fig. 10 that the rail discs tested under corrective maintenance conditions exhibit thicker WEL. This can be seen by comparing data between Fig. 8 and Fig. 11 which determines that the average WEL thickness is larger in rails ground in a corrective approach. The discs which were subjected to a preventive maintenance process have a thinner layer instead. This could have been caused by the excessive material that was removed on the single grinding pass. Moreover, the multiple passes experiments allowed the discs to cool down in-between passes. However, in single pass experiments the discs interacted with the grinding stone continuously, generating higher temperatures in the contact zone. Thus, it can be said that the single pass test in combination with higher material removal rates has caused an increased in WEL thickness.

In this set of experiments one of the main objectives was to identify the effect of WEL on the rail discs. The results showed clear indication that cracks near or/and within WEL implying that WEL can affect the life-cycle of the rail material. This suggested by other studies as well [20, 21] where it was stated that the martensite layer on top of the rail can cause crack formation on a post-grinding stage. This is clearly demonstrated in Fig. 16 and Fig. 21 where WEL could aided in the formation of cracks within the layer. As the martensite layer is harder than the bulk material it is more fragile as well. Any load applied to it can easily cause crack initiation and propagation leading to significant defects as shown in Fig. 21. The number of cracks observed in the various rail grades can be correlated with the surface roughness results from Fig. 13 b) and Fig. 18 b). This supports findings that suggested WEL has a low fracture toughness that makes it more prone to brittle failure compared to the undeformed pearlite [22]. Roughness values obtained during the twin-disc testing exhibited higher roughness for the harder rail materials in both the preventive and corrective maintenance method. A rough surface has more edges which in combination with the existence of WEL can result in crack formation as these spots act as stress concentration points. Similar results were observed by Steenbergen et al. [6].

Furthermore, it needs to be noted that the mechanism and energies involved in the laboratory testing is very different from the ones existing in the field with the main differences being the number of stones/

multiple facets and the configuration of the grinding process. Thus, it should be noted that these results are only an indication of similar features that can be observed in the field and not an exact representation of the field grinding process.

An article from the Technical University of Denmark [23] reinforces the previous argument as it states that an increased number of defects were found on head-hardened rail steel as a consequence of the aggressive grinding process. The track engineer interviewed stated that this forced the railway service provider to switch back to the less hard type of rail to minimise the number of defects. Although it does not specify the reason softer rails do not face similar problems it is clear that a similar phenomenon occurred with the softer rails being able to delaminate WEL easier, minimising the possibilities of crack formation due to grinding.

Comparing the wear rates between the corrective grinding experiments and preventive grinding it can be observed that the results from the corrective grinding set of experiments are higher apart from the MHH 375 and LC260. One can say that the increased wear rate is due to the corrective grinding process that took place prior to the twin-disc testing. The formation of larger quantities of WEL in combination with the accumulation of stress during the grinding process could be prime factors for this. During the initial run-in period the smoothing of the asperities takes place and the occasional fracture of some. Following the initial run-in, the tribo-system is attempting to reach a steady-state condition in a ratchetting type process. Throughout this stage the system was within the run-in/mild wear region based on work by Blau et al. [24]. Additionally, the brittle nature of WEL which leads to the formation of cracks and spallation of martensite could be a crucial factor for the increased wear rates observed. This was clearly observed in Fig. 16 and Fig. 21 martensite bands delaminate during the rolling/sliding loading leading to increased losses with regards to the material.

Another factor where particular attention needs to be given is the configuration of the small-scale grinding testing and post-grinding sliding/rolling testing. It should be stated that the energy and mechanics of the small-scale grinding testing as well as the rolling/sliding experiments performed in laboratory are not directly representative to the processes occurring in the field. However, with a relatively low cost it can produce results that could indicate features similar to those observed in the field such as comparable data. This was clearly demonstrated in another study [4] through a direct comparison between the laboratory results and field results performed under comparable conditions. Nevertheless, small-scale testing involves limitations in terms of simulation of field conditions but offer more control in terms of the grinding parameters where extensive studies can be made on the effect of grinding on rail microstructure.

5. Conclusions

Taking into account the data obtained from this set of experiments it can be said that the experimental methodology successfully simulates the conditions that exist in the field. The aim of assessing the performance of the rails upon the occurrence of grinding was successfully achieved.

The results, that were discussed thoroughly, have shown the effect of grinding processes on rail discs. The testing was split into two main groups where the grinding maintenance type and post-grinding performance were studied. For the grinding maintenance, two main methodologies were taken: corrective grinding and preventive grinding. Upon analysing the microstructure of the ground discs, it was concluded that the corrective maintenance process can generate a thicker more uniform and consistent WEL compared to preventive grinding. Moreover, from the twin-discs testing results it was identified that WEL can directly affect the formation of cracks and defects. Additionally, it was found that the harder grades retained larger quantities of WEL upon completion of the rolling/sliding testing due to the hardness gradient between the WEL and bulk material. This promoted the formation of cracks on the

specimens as the brittle nature of WEL can initiate cracks that propagate towards the bulk material.

Author statement

Michael Mesaritis: Conceptualization, Methodology, Software, Investigation, Data Curation, Writing – Original Draft, Writing-Review & Editing, Visualization, Project administration. **Paula Cuervo:** Data Curation. **Juan F. Santa:** Resources, Project administration. **Alejandro Toro:** Supervision, Funding acquisition, Project administration. **Roger Lewis:** Supervision, Funding acquisition, Resources, Project administration.

Declaration of competing interest

The authors declare that they have no known competing financial interests or personal relationships that could have appeared to influence the work reported in this paper.

Data availability

Data will be made available on request.

Acknowledgements

For the purpose of open access, the author has applied a 'Creative Commons Attribution (CC BY)*' licence to any Author Accepted Manuscript version arising. The authors are grateful to the Royal Academy of Engineering for financial support through the Industry Academia Partnership Programme, project n. IAPP\1516\91, Metro de Medellín for providing rails and wheels for study, and Network Rail for partially funding this study.

References

- [1] S.L. Grassie, Maintenance of the wheel-rail interface, in: *Wheel-Rail Interface Handbook*, Woodhead Publishing, 2009, pp. 576–607, <https://doi.org/10.1533/9781845696788.1.576>.
- [2] Metallography of steels. https://www.phase-trans.msm.cam.ac.uk/2008/Steel_Microstructure/SM.html. (Accessed 20 July 2020).
- [3] P. Christoforou, D.I. Fletcher, R. Lewis, Benchmarking of premium rail material wear, *Wear* 436–437 (Oct. 2019), 202990, <https://doi.org/10.1016/J.WEAR.2019.202990>.
- [4] M. Mesaritis, et al., A laboratory demonstration of rail grinding and analysis of running roughness and wear, *Wear* 456–457 (Jun. 2020), 203379, <https://doi.org/10.1016/j.wear.2020.203379>.
- [5] M. Mesaritis, J.F. Santa, L.F. Molina, M. Palacio, A. Toro, R. Lewis, Post-field grinding evaluation of different rail grades in full-scale wheel/rail laboratory tests, *Tribol. Int.* 177 (Jan. 2023), 107980, <https://doi.org/10.1016/J.TRIBOINT.2022.107980>.
- [6] M. Steenbergen, Rolling contact fatigue in relation to rail grinding, *Wear* 356 (357) (2016) 110–121, <https://doi.org/10.1016/j.wear.2016.03.015>.
- [7] J.F. Santa, et al., Twin disc assessment of wear regime transitions and rolling contact fatigue in R400HT – E8 pairs, *Wear* 432–433 (Aug. 2019), 102916, <https://doi.org/10.1016/j.wear.2019.05.031>.
- [8] J.F. Santa, A. Toro, R. Lewis, Correlations between rail wear rates and operating conditions in a commercial railroad, *Tribology International* 95 (2016) 5–12, <https://doi.org/10.1016/j.triboint.2015.11.003>.
- [9] O. Arias-Cuevas, Z. Li, R. Lewis, Investigating the lubricity and electrical insulation caused by sanding in dry wheel–rail contacts, *Tribol. Lett.* 37 (3) (Mar. 2010) 623–635, <https://doi.org/10.1007/s11249-009-9560-1>.
- [10] S.R. Lewis, R. Lewis, J. Cotter, X. Lu, D.T. Eadie, A new method for the assessment of traction enhancers and the generation of organic layers in a twin-disc machine, *Wear* 366 (367) (Nov. 2016) 258–267, <https://doi.org/10.1016/J.WEAR.2016.04.030>.
- [11] C. Esveld, *Modern Railway Track PREFACE I Modern Railway Track*, 2017 [Online]. Available: www.esved.com. (Accessed 28 February 2023).
- [12] S.R. Lewis, et al., Improving rail wear and RCF performance using laser cladding, *Wear* 366 (367) (Nov. 2016) 268–278, <https://doi.org/10.1016/J.WEAR.2016.05.011>.
- [13] S. Fukagai, H.P. Brunskill, A.K. Hunter, R.S. Dwyer-Joyce, R. Lewis, Transitions in rolling-sliding wheel/rail contact condition during running-in, *Tribol. Int.* 17 (2019), <https://doi.org/10.1016/j.triboint.2019.03.037> online.
- [14] D. C. Hill and D. E. Passoja, "Understanding the Role of Inclusions and Microstructure in Ductile Fracture Effects of Welding Process Variations on Toughness Are Best Understood by Studying the Weldment Microstructure and Inclusion Size Distribution".
- [15] Y. Zhou, J. liang Mo, Z. bing Cai, C. guang Deng, J. fang Peng, M. hao Zhu, Third-body and crack behavior in white etching layer induced by sliding–rolling friction, *Tribol. Int.* 140 (Dec. 2019), 105882, <https://doi.org/10.1016/j.triboint.2019.105882>.
- [16] E.L. Dalibón, L. Escalada, S. Simison, C. Forsich, D. Heim, S.P. Brühl, Mechanical and corrosion behavior of thick and soft DLC coatings, *Surf. Coat. Technol.* 312 (Feb. 2017) 101–109, <https://doi.org/10.1016/J.SURFCOAT.2016.10.006>.
- [17] B. Podgornik, et al., Tribological properties of plasma nitrided and hard coated AISI 4140 steel, *Wear* 249 (3–4) (May 2001) 254–259, [https://doi.org/10.1016/S0043-1648\(01\)00564-6](https://doi.org/10.1016/S0043-1648(01)00564-6).
- [18] J. Robertson, Diamond-like amorphous carbon, *Mater. Sci. Eng. R Rep.* 37 (4–6) (May 2002) 129–281, [https://doi.org/10.1016/S0927-796X\(02\)00005-0](https://doi.org/10.1016/S0927-796X(02)00005-0).
- [19] A.A. Candido Recco, A.P. Tschiptschin, Structural and mechanical characterization of duplex multilayer coatings deposited onto H13 tool steel, *J. Mater. Res. Technol.* 1 (3) (Oct. 2012) 182–188, [https://doi.org/10.1016/S2238-7854\(12\)70031-5](https://doi.org/10.1016/S2238-7854(12)70031-5).
- [20] C.J. Rasmussen, S. Fæster, S. Dhar, J.V. Quaade, M. Bini, H.K. Danielsen, Surface crack formation on rails at grinding induced martensite white etching layers, *Wear* 384–385 (2017) 8–14, <https://doi.org/10.1016/j.wear.2017.04.014>. March.
- [21] D. Zapata, J.F. Santa, J.C. Sánchez, J.C. González, A. Toro, Effect of rail grinding conditions on sub-surface microstructure and surface roughness of fatigued rails, *Tecnología em Metalurgia, Materiais e Mineração* 20101124 (2010) 277–286.
- [22] A.K. Saxena, A. Kumar, M. Herbig, S. Brinckmann, G. Dehm, C. Kirchlechner, Micro fracture investigations of white etching layers, *Mater. Des.* 180 (Oct. 2019), 107892, <https://doi.org/10.1016/J.MATDES.2019.107892>.
- [23] New knowledge will change rail maintenance - DTU. <https://www.dtu.dk/english/news/2019/04/new-knowledge-will-change-rail-maintenance?id=4fdc348a-a205-4f98-931b-98fe5bdfa11a>. (Accessed 22 November 2021).
- [24] P.J. Blau, A model for run-in and other transitions in sliding friction, *J. Tribol.* 109 (3) (2009) 537, <https://doi.org/10.1115/1.3261499>.